

## Supporting Information

### **Substrate specificity in decarboxylation of mixtures of acetate and propionate using oxidized Pt electrodes and galvanic square-wave pulsed electrolysis**

Margot Olde Nordkamp,<sup>a</sup> Talal Ashraf,<sup>a</sup> Guido Mul,<sup>a,\*</sup> Bastian Timo Mei<sup>a,b,\*</sup>

<sup>a</sup>Photocatalytic Synthesis Group, Faculty of Science & Technology of the University of Twente, PO  
Box 217, Enschede, The Netherlands

<sup>b</sup>Technische Chemie, Ruhr-Universität Bochum, Universitätsstr. 150, 44801 Bochum, Germany

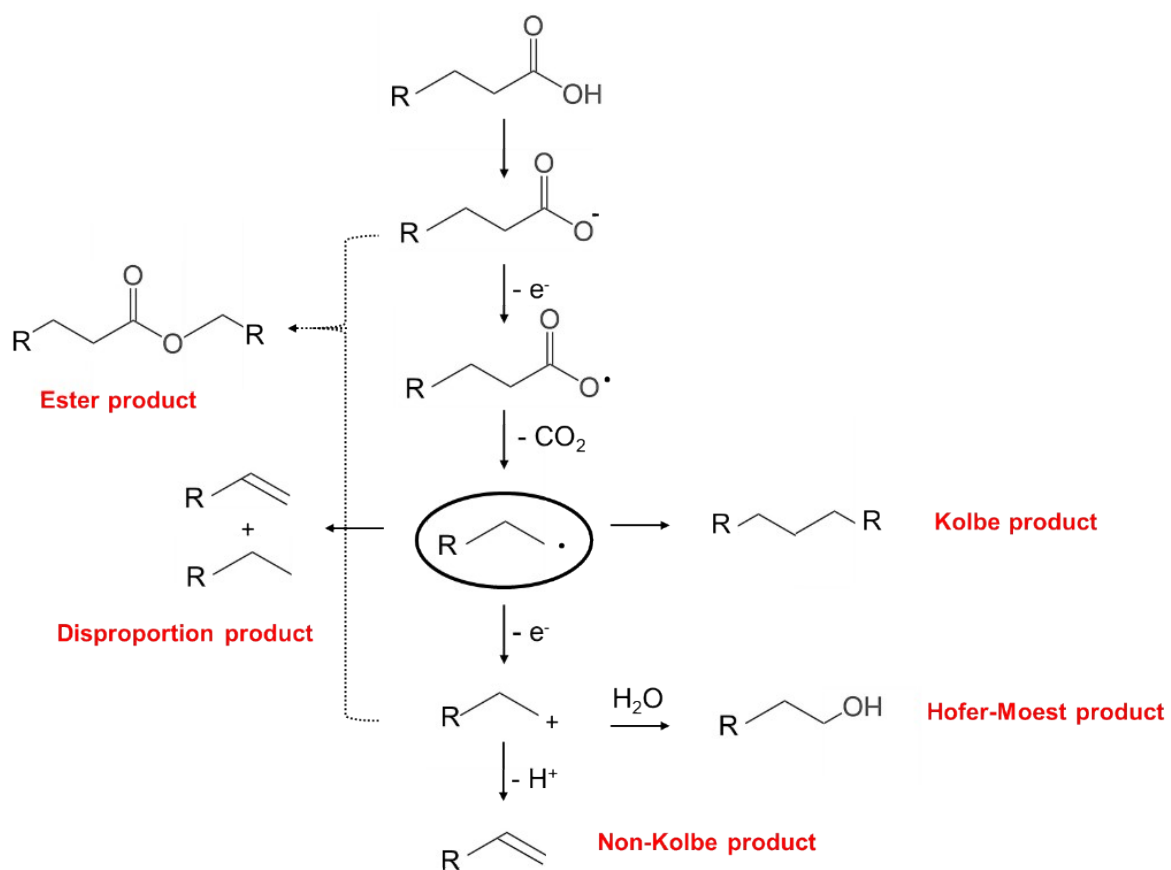


**Figure S1** Schematic representation of the reaction mechanism for the formation of Kolbe, Hofer-Moest, Non-Kolbe, disproportionation and ester products.

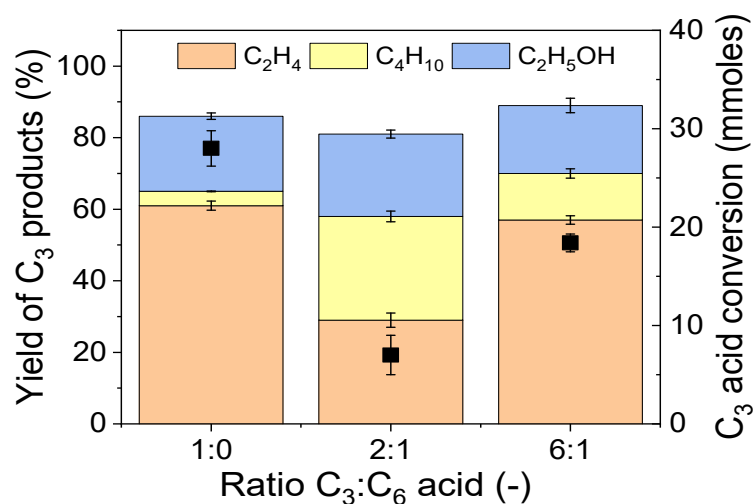


**Figure S2.** Faradaic Efficiency (%) to ethylene, butane, ethanol and other products during Kolbe electrolysis of mixtures of propionic acid (C3) and hexanoic acid (C6) with different ratios. The second y-axis shows the conversion (in mmoles) of propionic acid (black squares) after 5000 C of charge passed. The electrolyte pH was maintained between pH 6-8, the total acid concentration was 1 M and the applied current density was 250 mA/cm<sup>2</sup>. The error margins are based on N=2.

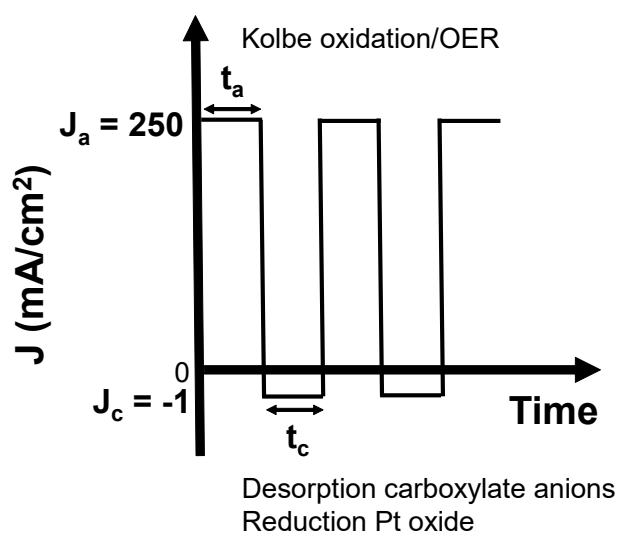


**Figure S3.** Schematic representation of galvanic square wave pulses, with an anodic current density ( $J_a$ ) of 250 mA/cm<sup>2</sup> and cathodic current density ( $J_c$ ) of -1 mA/cm<sup>2</sup>.  $t_a$  and  $t_c$  present the duration of the anodic and cathodic pulse, respectively.

Upon applying the negative cathodic pulse, Kolbe electrolysis is interrupted. Carboxylate anions desorb from the platinum electrode surface by the opposing charge, which leads to the disruption of the carboxylate layer. Additionally, oxidation of the Pt surface oxide will occur. During the positive anodic pulse, the conditions for Kolbe electrolysis will restore again.

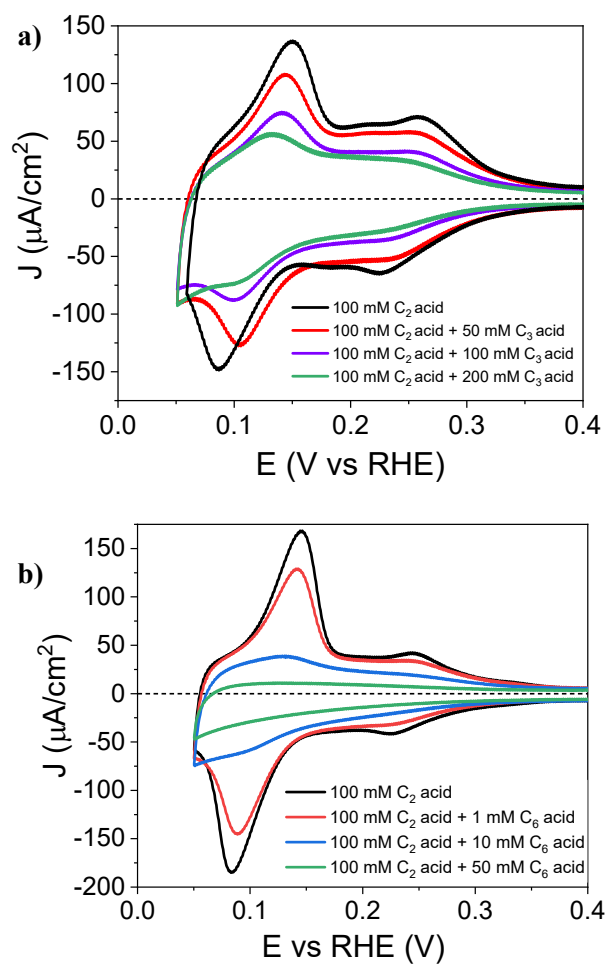


**Figure S4.** a) Cyclic voltammograms showing hydrogen underpotential deposition of 50, 100 and 200 mM  $\text{C}_3$  acid in 100 mM  $\text{C}_2$  acid buffer b) 1, 10 and 50 mM  $\text{C}_6$  acid in 100 mM  $\text{C}_2$  acid buffer at 100 mV/s at room temperature.

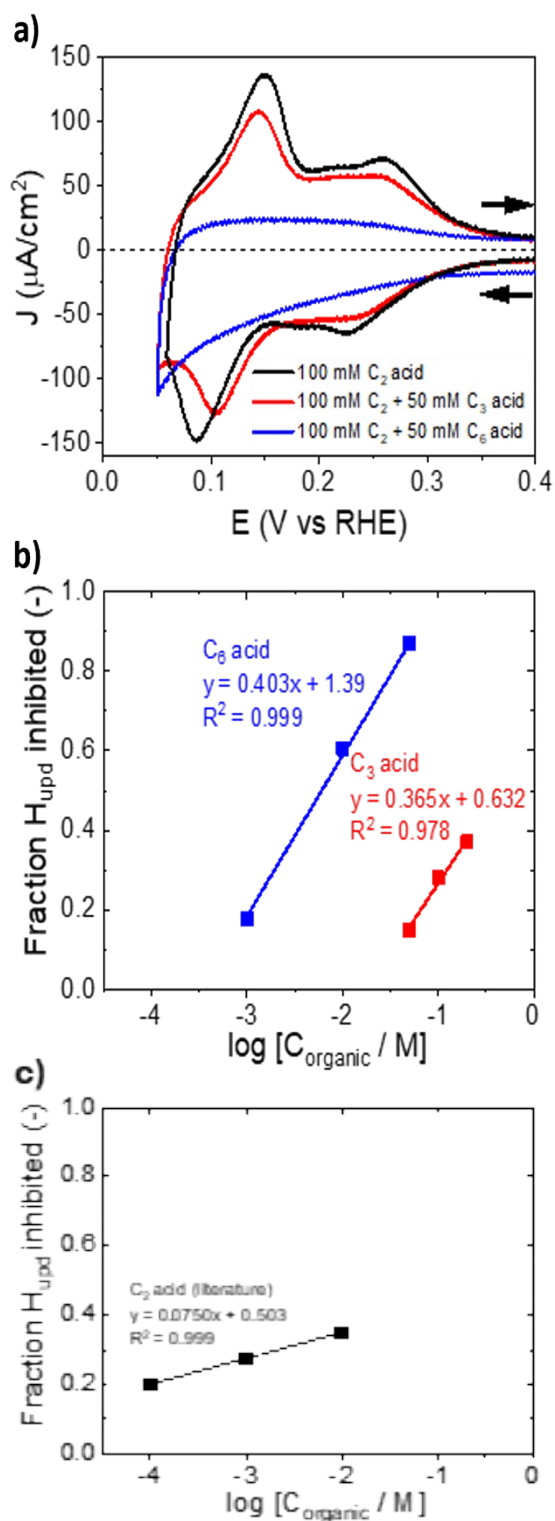


**Figure S5.** a) Cyclic voltammogram on Pt electrodes in 50 mM  $\text{C}_3$  acid (red trace) and 50 mM  $\text{C}_6$  acid (blue trace) in 100 mM  $\text{C}_2$  acid buffer. Measurements are performed at a scan rate of 100 mV/s at room temperature. The potential window was adjusted to highlight differences in the hydrogen underpotential deposition voltage range. b) Temkin adsorption isotherm extracted from CV measurements performed with electrolytes of different  $\text{C}_3$  and  $\text{C}_6$  acid concentrations. All measurements are referred to CVs obtained in a  $\text{C}_2$  buffer and extracted from the original datasets shown in Figure S3. c) Temkin adsorption isotherm of  $\text{C}_2$  acid in 1 M  $\text{HClO}_4$  electrolyte. The data for the Temkin isotherm of  $\text{C}_2$  acid was extracted from adsorption data provided in the work of Gilman et al., see main article reference [34].